

Point cloud completion on structured feature map with feedback network

Zejia Su¹, Haibin Huang², Chongyang Ma², Hui Huang¹, and Ruizhen Hu¹ (✉)

© The Author(s) 2022. This article is published with open access at Springerlink.com

Abstract In this paper, we tackle the challenging problem of point cloud completion from the perspective of feature learning. Our key observation is that to recover the underlying structures as well as surface details given a partial input, a fundamental component is a good feature representation that can capture both global structure and local geometric details. Towards this end, we first propose FSNet, a feature structuring module that can adaptively aggregate point-wise features into a 2D structured feature map by learning multiple latent patterns from local regions. We then integrate FSNet into a coarse-to-fine pipeline for point cloud completion. Specifically, a 2D convolutional neural network is adopted to decode feature maps from FSNet into a coarse and complete point cloud. Next, a point cloud upsampling network is used to generate dense point cloud from the partial input and the coarse intermediate output. To efficiently exploit the local structures and enhance the point distribution uniformity, we propose IFNet, a point upsampling module with self-correction mechanism that can progressively refine details of the generated dense point cloud. We conduct both qualitative and quantitative experiments on ShapeNet, MVP, and KITTI datasets, which demonstrate that our method outperforms state-of-the-art point cloud completion approaches.

Keywords 3D point clouds; shape completion; geometry processing; deep learning.

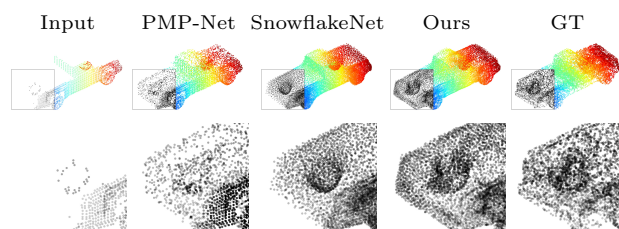


Fig. 1 Our approach can generate point cloud completion result from partial input with finer details and more uniform surface points compared to state-of-the-art methods.

1 Introduction

In this paper, we study the problem of point cloud completion, i.e. recovering a full point cloud given a partial observation. It is an important component in many real-world applications, such as 3D data scanning [2], acquisition [28], robot navigation [15] and so on.

Point cloud completion has been proven to be a quite challenging task as it needs to recover both the missing topology structures and geometry details from incomplete input. Traditional methods [3, 19] used hand-crafted features like surface smoothness or symmetric priors. Such empirical human-designed features would suffer from performance degeneration with changing illuminations and severe occlusions. Recently, Deep Neural Network (DNN) based methods have been introduced into this task and have achieved promising improvements. Early works [4, 27] voxelize the 3D point cloud and apply 3D Convolutional Neural Network(CNN) on the volumetric data to complete the shapes. Due to the large computational cost of 3D CNN, such methods generally output shapes with limited details. Pioneered by PointNet [22] and PointNet++ [23], there are more methods [29, 47] that directly worked on 3D point cloud for completion. Compared with voxels, learning on 3D points is more scalable and efficient, but also leads to the problem of

1 Shenzhen University, Shenzhen, China. E-mail: zejiasu.36@gmail.com, hhzhian@gmail.com, ruizhen.hu@gmail.com (✉).

2 Kuaishou Technology, China. E-mail: jackiehuanghaibin@gmail.com, chongyangm@gmail.com.

Manuscript received: 2014-12-31; accepted: 2015-01-30.

feature learning due to the inherent irregularity and sparseness of point cloud.

A common practice for previous methods is to apply MLPs for point cloud via an encoder-decoder manner, where per-point features are aggregated to a global feature vector via the max-pooling operation and then decoded into a complete point cloud. Due to the involving of pooling operation, these methods suffer from unavoidable information loss which results in unsatisfactory shape structures and blurry details in the missing regions. More recently, there are methods proposed to improve the feature learning, including shape priors [21], skip-attention mechanism [36], and so on [42, 49]. However, most of these methods adopt feature vector as the global representation and suffer from non-uniform distribution in the dense prediction results, due to the irregular and discrete nature of point cloud, especially when the input shapes have large missing parts. As shown in Fig. 1, the distributions of the point clouds predicted by previous methods are uneven such as those regions between the known and predicted parts.

To tackle these challenges, we propose a new point cloud completion method with two novel modules, i.e., FSNet for structured feature learning which captures well both global structure and local geometric details of input point cloud, as well as IFNet for progressively detail generation and uniformity enhancement. Given a partial input, point-wise feature is first extracted by an encoder and FSNet is then applied to form a 2D structured feature map. Instead of max-pooling operation, FSNet relies on multi-head attention [30] to aggregate the features, where a learnable set and the input features are used as queries and key-value pairs, respectively, and the output matrices constitute the structured feature map. By exploiting latent patterns among local regions, FSNet can learn a global representation with rich semantic information to be distinguishable at the instance level. The 2D structured feature map then allows us to utilize a 2D Convolutional Neural Network as a decoder to predict the complete structures and generate a coarse point cloud as the input of the upsampling stage. Motivated by the success of feedback mechanism in image super-resolution task [9], we further propose IFNet with self-correction strategy to upsamples the coarse point cloud in a progressive manner. In practice of the upsampling stage, a sparse encoding module is applied to extract sparse feature from the coarse point cloud and input, and followed by a upsampling module to generate initial dense features. The final dense point cloud is then

iteratively refined through IFNet, where the details are progressively added and the uniformity is gradually improved by feeding back the projection error to the initial dense features.

We conduct experiments on ShapeNet, MVP and KITTI datasets to evaluate our method. Experimental results show that our approach can outperform state-of-the-art methods.

To summarize, our contributions are as follows:

- We propose FSNet, a novel feature aggregation network to adaptively organize the unordered features into a 2D structured feature map, which can retain more information and represent more fine-grained global feature compared to a feature vector;
- We design IFNet, an iterative feedback network to upsample and refine the coarse completion via multi-step self-correction procedure, which can further exploit the local details and facilitate the consolidation and uniformity of point cloud;
- We evaluate different algorithms on both synthetic and real-world datasets and show that our approach outperforms state-of-the-art methods in terms of both completion quality and surface uniformity.

2 Related Work

3D shape completion. 3D shape completion has drawn increasing attention in recent years. Early geometry-based methods [3, 19] complete the objects by leveraging predefined geometric features, such as surface smoothness or symmetric priors. Since these methods rely on hand-crafted features, they are only valid under particular circumstances. Recently, Convolutional Neural Network (CNN) has been widely used to processing regularly arranged data due to its ability of feature learning. There are some methods [4, 27] introduce 3D voxel grids or distance fields as the representation for 3D data, and utilize 3D CNN to complete the objects. However, the use of 3D CNN leads to large computation and memory cost that are cubic to the resolution of the volumetric data, and the reduction in the resolution limits the processing of fine-grained shapes.

Recent works tend to adopt 3D point cloud as the representation of 3D objects due to its convenience and flexibility. Pioneered by pointnet [22], several methods use MLPs for point cloud completion under an encoder-decoder framework, where per-point features are aggregated to a global feature vector (GFV) by the max-pooling operation. PCN [47] and

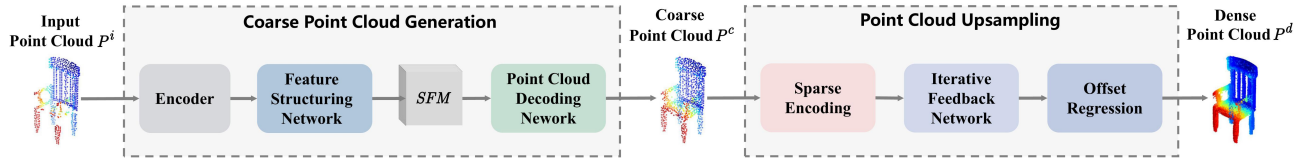


Fig. 2 An illustration of the overall pipeline.

MSN [18] complete the point cloud in a coarse-to-fine fashion. TopNet [29] introduce a hierarchical tree-structure network that takes the geometric structure into consideration. RL-GAN-Net [26] and Render4Completion [10] focused on the framework of adversarial learning to improve the reality and consistency of the generated shape. However, these methods suffer from the loss of structure details, as they predict the point cloud only from a single global vector.

To better preserve shape structures and complete surface details, SA-Net [36] and ASHF-Net [51] introduce a skip-attention mechanism to further revisit the low-level features from the encoder. SoftpoolNet [34] proposes a soft pooling module to replace max-pooling operator, which can keep more information by considering multiple features. NSFA [49] aggregates different features to represent the known part and the missing part separately. GRNet [42] and VE-PCN [31] introduce 3D voxels as the intermediate representation to aid the network to infer the the complete shape. PF-Net [11], DeCo [1], and PoinTr [46] only generate the missing part of the object to preserve the spatial arrangements of the original part. VRCNet [21] and ASFM-Net [39] improve the global features by narrow the distribution difference between the incomplete and complete point cloud. CRN [32] and SnowflakeNet [40] generate the complete point cloud following in a progressive manner. Other notable work such as PMP-Net [37] formulate the completion as a point cloud deformation process, where point-wise moving paths are predicted to move each point of the incomplete input to complete the point cloud. SpareNet [41] proposes a style-based point generator with adversarial rendering for point cloud completion. Cycle4Completion [35] improves the completion quality by establishing the geometric correspondence between complete shapes and incomplete ones.

Point cloud upsampling. Point cloud upsampling aims to generate a uniform dense point cloud to represent the underlying surface of the object within local patches. PU-Net [45] uses PointNet++ [23] to

extract multi-scale features and expands the features through multi-branch MLPs. With additional edge and surface annotations, EC-Net [44] improve the edge quality of PU-Net by formulating edge-aware joint loss to learn geometry of edges. MPU [43] proposes a progressive network to upsample points in multi-stages, which requires supervision on intermediate outputs. PU-GAN [17] presents a Generative Adversarial Network (GAN) to learn the distribution of dense point cloud. PUGeo-Net [25] proposes a geometric-centric network by learning local parameterization and normal direction for each point, which needs addition normal annotations. Recently, PU-GCN [24] designs a novel feature expansion network called NodeShuffle, which utilizes Graph Convolutional Networks (GCNs) to encode local information.

3 Method

In this section, we formally introduce our proposed method. As shown in Fig. 2, we present a two-stage pipeline which works in a coarse-to-fine manner and consists of a coarse structure completion stage and a point cloud upsampling stage. More specifically, taking a partial point cloud $P^i \in \mathbb{R}^{N^i \times 3}$ as input, a novel feature structuring module FSNet is firstly introduced, which aggregates point-wise features encoded from P^i into a 2D structured feature map SFM and feeds it to a point cloud decoding network to produce a coarse point cloud $P^c \in \mathbb{R}^{N^c \times 3}$, where N^i and N^c denote the numbers of partial input points and coarse completion points, respectively. Then, a sparse encoding module and a novel iterative feedback network IFNet are applied sequentially to upsample and refine the coarse completion P^c , followed by a offset regression module to obtain a dense point cloud $P^d \in \mathbb{R}^{N^d \times 3}$ with fine-grained details, where N^d denotes the number of dense completion points.

3.1 Coarse Point Cloud Generation

The goal of the first stage is to generate a coarse and complete point cloud. The main challenge is how to recover a coarse shape that is correct in global structures while maintaining sufficient local

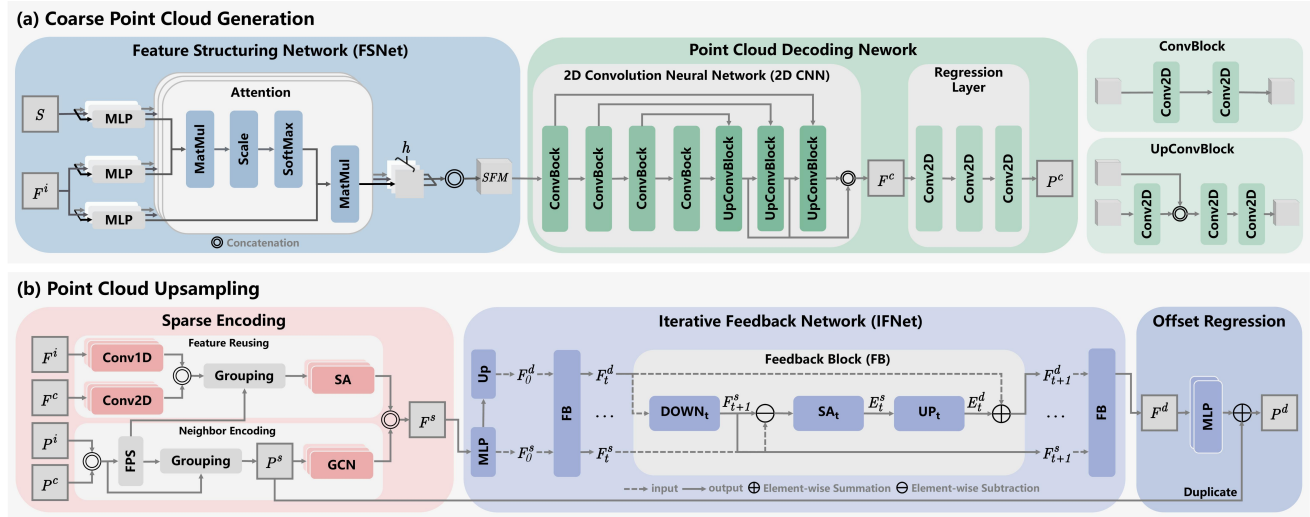


Fig. 3 The network architectures of (a) our coarse point cloud generation module and (b) our point cloud upsampling module.



Fig. 4 Visualization of the normalized attention weights of some representative channels in SFM .

geometric details w.r.t the input. To this end, we propose feature structuring network (FSNet) that can adaptively aggregate point-wise features into a 2D feature map and then decode it into a coarse point cloud, as shown in Fig. 3 (a).

Feature structuring network. To preserve permutation invariant of points in the input, max pooling is wildly used in previous methods and often leads to unavoidable information loss of local details. Inspired by Set Transformer [16], we propose FSNet, which utilizes multi-head attention [30] instead of max pooling to aggregate point-wise features in a data-driven way and keep irrelevant to the order of the input points.

Specifically, given point-wise features $F^i \in \mathbb{R}^{N^i \times C^i}$ extracted from the input point cloud, we explore the latent patterns among local regions via attention mechanism. We first define a learnable set with k vectors $S \in \mathbb{R}^{k \times C^i}$ and the F^i as the queries and key-value pairs. Then, we linear project the queries, keys and values h times through different MLPs to dimension d . We further perform attention function [30] on the projected features, yielding h matrices with a shape of $k \times d$, where each matrix is generated by the weighed sum of the projected

input features and the attention weights can imply the geometrical region that the corresponding channel extracted from input point cloud. These matrices are then concatenated together to generate a 2D structured feature map $SFM \in \mathbb{R}^{h \times k \times d}$ with a shape of $k \times d$ and h channels. Note that the output feature map is irrelevant to the order of the input points, and naturally takes all the vectors of input features into consideration thanks to the attention mechanism.

To have a better understanding of the learned SFM, we first visualize the normalized attention weights of some representative channels using the hot colormap in Fig. 4. We observe that the distribution of attention weights show different patterns across channels, and some of them reveal semantic correlation, while others are geometric complementary, indicating the structured feature map contains different combinations of local information from the input point cloud.

Point cloud decoding network. With the learned SFM, the next step is to generate a coarse but complete point cloud that can recover the overall structure of the target object. The key challenge here is to be able to infer the features of missing regions and recover the underlying structure with diverse topology. Our key observation is that since SFM is in 2D regular format and contains rich local information of the input, it enables us to model the point cloud structure via the 2D convolution operations. So we build a decoding network that learns to generate a point cloud from SFM, and it is composed of two parts: a 2D CNN with UNet structure and a regression layer. In more details, given SFM as input, the 2D CNN produces the

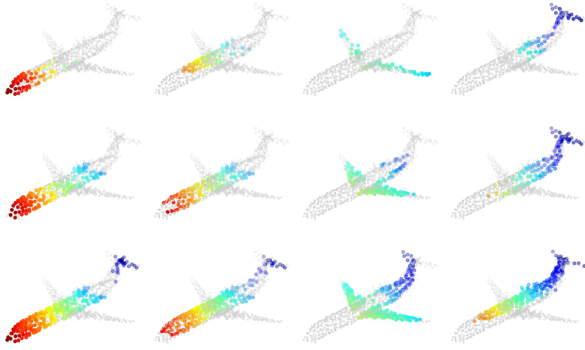


Fig. 5 Visualization of representative structures learned by the decoding network. Local patches in the 2D structured point cloud \bar{P}^c correspond to local point regions, and the point regions keep growing with the increase of patch size from the top row to the bottom row.

coarse features $F^c \in \mathbb{R}^{C^c \times k \times d}$, and then the regression layer transforms F^c to an intermediate output \bar{P}^c with shape $3 \times (k/2) \times (d/2)$, which is reshaped to form the corresponding coarse point cloud $P^c \in \mathbb{R}^{N^c \times 3}$.

Note that as the structure information is implicitly modeled in the 2D CNN, local patches in \bar{P}^c actually correspond to local neighboring point regions, which represent the local structure of the object. Fig. 5 shows some example local point regions corresponding to local patches in \bar{P}^c with increasing sizes from top row to the third row, where we use a sliding window with different sizes to extract the local patches. We can see that the point regions corresponding to smaller patches represent the low-level structures of the object, and point regions keep growing with the increase of local patch size in \bar{P}^c to represent the high-level structures of the object, which shows that the CNN-based decoding network can precisely model the structure of point cloud with the given SFM.

3.2 Point Cloud Upsampling

After generating the coarse point cloud P^c , a point cloud upsampling stage is followed to produce a dense point cloud P^d with fine-grained details and uniform distribution. As illustrated in Fig. 3 (b), our proposed point cloud upsampling stage can be divided into three steps, i.e., sparse encoding, feature expansion, and offset regression.

Sparse encoding. The first step is a sparse encoding module which servers as sparse feature preparation and provides both local and contextual information to following steps. It consists of two branches: a neighbor encoding path to preserve the geometric

structures, and a feature reusing path to explore the structure details on local regions by revisiting the input features F^i and coarse features F^c . For neighbor encoding path, we first combine P^c with P^i , followed by farthest point sampling and grouping operation, which produces a sparse and relatively uniform point cloud $P^s \in \mathbb{R}^{N^s \times 3}$, where N^s denotes the number of sparse sampled points. We then follow the GCNs structure in DGCNN [33] with adaption of EdgeConv [33] as the GCN layer, which sequentially aggregate features from the local neighbors for each point. For feature reusing path, F^i and F^c are passed to a sequence of 1D and 2D convolution layers separately. The output features are concatenated together, followed by a grouping operation and a sequence of self-attention units [48] to enhance the feature integration. At the end, features from the two paths are concatenated as the sparse features $F^s \in \mathbb{R}^{N^s \times C^s}$ and fed into the feature expansion step.

Iterative feedback network. Inspired by DBPN [9] from the image super resolution tasks, we introduce a feedback mechanism into feature expansion by constructing an Iterative Feedback Network (IFNet) that can effectively expand the sparse features through multi-step refinement. The network first reduce the dimension of F^s from C^s to c by a MLPs and expand it through an upsampling unit, producing the initial sparse features $F_0^s \in \mathbb{R}^{N^s \times c}$ and dense point features $F_0^d \in \mathbb{R}^{rN^s \times c}$, where r denotes the upsampling ratio. It then feeds the initial features into a sequence of Feedback Blocks (FB) to perform self-correction procedures.

To be more specific, a feedback block is consisted with upsampling unit, downsampling unit and self-attention unit, which is defined as:

$$\text{scale down : } F_{t+1}^s = \text{DOWN}_t(F_t^d, r) \quad (1)$$

$$\text{difference : } E_t^s = \text{SA}_t(F_{t+1}^s - F_t^s) \quad (2)$$

$$\text{scale difference up : } E_t^d = \text{UP}_t(E_t^s, r) \quad (3)$$

$$\text{corrected features : } F_{t+1}^d = F_t^d + E_t^d \quad (4)$$

where SA denotes the self-attention unit [48], and UP(F, r) and Down(F, r) denote the upsampling and downsampling operation on features F with a ratio r , respectively. Detailed network architectures are shown in the supplementary materials.

Each feedback block takes sparse features $F_t^s \in \mathbb{R}^{N^s \times c}$ and dense features $F_t^d \in \mathbb{R}^{rN^s \times c}$ as inputs, and maps the dense features F_t^d to a new sparse features $F_{t+1}^s \in \mathbb{R}^{N^s \times c}$. The difference $E_t^s \in \mathbb{R}^{N^s \times c}$ between known sparse features F_t^s and the reconstructed sparse

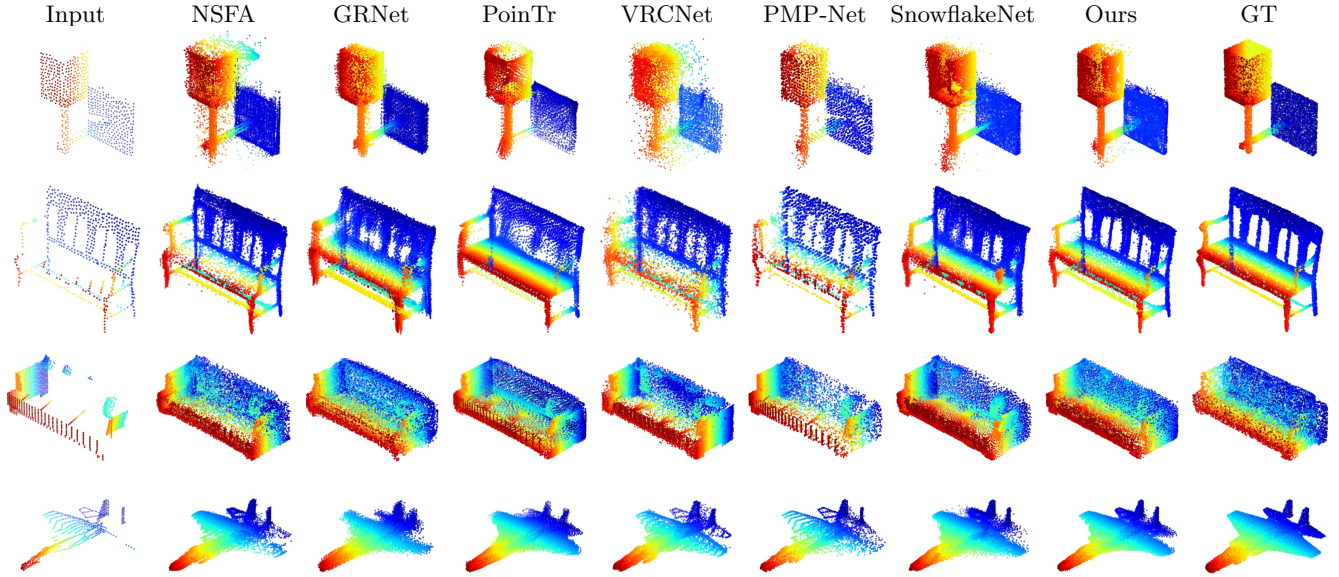


Fig. 6 Qualitative completion results on ShapeNet dataset.

features F_{t+1}^s is computed, followed by a self-attention unit to produce more discriminative error by capturing long-range contextual information. After that, the difference is mapped to a intermediate dense features $E_t^d \in \mathbb{R}^{rN^s \times c}$, and the corrected dense features $F_{t+1}^d \in \mathbb{R}^{rN^s \times c}$ are obtained by adding E_t^d to F_t^d . Intuitively, each block performs a self-correction procedure by feeding back the projection error to the initial dense features and enables the networks to produce dense features that are favour of the regression of dense point cloud with fine-grained details and uniform distribution.

Offset regression. In the last process, we generate the dense point cloud P^d based on the produced dense features $F^d \in \mathbb{R}^{N^d \times c}$ by predicting offsets between the coordinates of points in the sparse and dense point cloud, where the residual offsets are regressed through two layers of MLPs and the sparse point cloud P^s is replicated r times before residual summation. Note that the number of dense completion points $N^d = rN^s$.

3.3 Loss function

We choose Chamfer distance (CD) as the reconstruction loss due to its efficiency. Following PS2Net [5] and TopNet [29], the Chamfer Distance

between two point set X and Y is defined as:

$$L_{CD}(X, Y) = L_{X, Y} + L_{Y, X}, \text{ where}$$

$$L_{X, Y} = \frac{1}{|X|} \sum_{x \in X} \min_{y \in Y} \|x - y\|_2^2, \text{ and}$$

$$L_{Y, X} = \frac{1}{|Y|} \sum_{y \in Y} \min_{x \in X} \|x - y\|_2^2 \quad (5)$$

Since we generate the complete point cloud in a coarse-to-fine fashion, we jointly optimize the coarse point cloud P^c and dense point cloud P^d via the CD loss. The overall training loss is defined as:

$$L = L_{CD}(P^s, P^g) + L_{CD}(P^d, P^g) \quad (6)$$

where $P^g \in \mathbb{R}^{N^g \times 3}$ denotes the ground truth point cloud, and N^g denotes the number of ground truth points.

4 Experiments

4.1 Datasets

We evaluate our method in three popular benchmarks, including ShapeNet [38], MVP [21], and KITTI [6]. The details of each dataset are listed as below:

ShapeNet. The ShapeNet dataset for point cloud completion is derived from PCN [47], in which 30,974 samples are selected from 8 categories. The ground truth point clouds containing 16,384 points are uniformly sampled on mesh surfaces. The partial point clouds are generated by back-projecting 2.5D depth maps from 8 random views into 3D. For a fair

Tab. 1 Shape completion results (CD loss multiplied by 10^4) on ShapeNet dataset.

Methods	Plane	Cabinet	Car	Chair	Lamp	Sofa	Table	Vessel	Avg.
PCN [47]	1.40	4.45	2.45	4.84	6.24	5.13	3.57	4.06	4.02
TopNet [29]	2.15	5.62	3.51	6.35	7.50	6.95	4.78	4.36	5.15
MSN [18]	1.54	7.25	4.71	4.54	6.48	5.89	3.80	3.85	4.76
NSFA [49]	1.75	5.31	3.43	5.01	4.73	6.41	4.00	3.56	4.27
PF-Net [11]	1.55	4.43	3.12	3.96	4.21	5.87	3.35	3.89	3.80
CRN [32]	1.46	4.21	2.97	3.24	5.16	5.01	3.99	3.96	3.75
GRNet [42]	1.53	3.62	2.75	2.95	2.65	3.61	2.55	2.12	2.72
PoinTr [46]	0.99	4.80	2.52	3.68	3.07	6.53	3.10	2.02	3.34
VRCNet [21]	1.53	4.66	2.66	4.62	5.50	5.70	4.39	3.58	4.08
PMP-Net [37]	1.22	4.18	2.85	3.51	2.14	4.22	2.89	1.88	2.86
SnowflakeNet [40]	0.86	3.40	2.36	2.68	2.06	4.46	2.16	1.74	2.47
ASHF-Net [51]	1.40	3.49	2.32	2.82	2.52	3.48	2.42	1.99	2.55
Ours	0.80	3.53	2.13	2.48	1.79	3.64	1.98	1.81	2.27

comparison, we use the same train/val/test splits as PCN.

MVP. The MVP dataset consists of 16 categories of partial/complete point clouds that are generated by CAD-model selected from ShapeNet dataset [38], where there are 62,400 and 41600 shape pairs in training set and testing set, respectively. Unlike other dataset, the complete point cloud in MVP has different resolutions, including 2048, 4096, 8192 and 16384, which can be used to evaluate the completion quality at different resolutions. We use the same train/test splits as in VRCNet [21] to evaluate our method.

KITTI. The KITTI dataset is composed of a sequence of real-world LiDAR scans, also derived from PCN [47]. For each frame, the car point cloud are extracted within the object bounding boxes labeled as car, resulting in 2,401 partial point clouds, and there are no ground truth exist in the dataset.

4.2 Implementation Details

We use DGCNN [33] as the encoder to extract features from the input point cloud. Both d and k are set to 64 for generating a coarse completion P^c with $N^c = 1024$ points. The number of channel h of SFM is set to 32 according to the ablation study. We typically sample $N^s = 1024$ points to obtain the sparse point cloud P^s , which is sufficient to cover the overall structures of the objects. Besides, we can generate dense output P^d with various resolutions, including $N^d = 2048, 4096, 8192, 16384$, where the upsampling ratio r is set to 2, 4, 8, and 16, respectively.

Our networks are implemented using PyTorch and optimized using an Adam optimizer [13] with $\beta_1 = 0.9$

Tab. 2 Shape completion results (CD loss multiplied by 10^4 and F-score@1%) with various resolutions on MVP dataset.

Points	2,048		4,096		8,192		16,384	
	CD	F1	CD	F1	CD	F1	CD	F1
PCN [47]	9.77	0.320	7.96	0.458	6.99	0.563	6.02	0.638
TopNet [29]	10.11	0.308	8.20	0.440	7.00	0.533	6.36	0.601
MSN [18]	7.90	0.432	6.17	0.585	5.42	0.659	4.90	0.710
CRN [32]	7.25	0.434	5.83	0.569	4.90	0.680	4.30	0.740
ECG [20]	6.64	0.476	5.41	0.585	4.18	0.690	3.58	0.753
VRCNet [21]	5.96	0.499	4.70	0.636	3.64	0.727	3.12	0.791
PMPNet [37]	6.33	0.479	4.63	0.584	3.52	0.680	2.79	0.753
SnowflakeNet [40]	6.06	0.500	4.80	0.615	3.49	0.739	2.75	0.805
Ours	5.53	0.503	4.20	0.648	3.19	0.760	2.33	0.810

and $\beta_2 = 0.999$. The initial learning rate is $1e^{-3}$ and is multiplied by 0.7 per 10 epochs. We train the networks with a batch size of 32 on four NVIDIA TITAN Xp GPUs.

4.3 Comparisons with State-of-the-Arts

We compare our method against several State-of-the-Arts works, with both quantitative results and visual comparisons.

Results on ShapeNet. The quantitative results of our method with the other state-of-the-art point cloud completion methods on ShapeNet dataset is shown in Tab. 1, where our method outperforms all competitive methods in terms of the average CD across all the categories. Qualitative results are shown in Fig. 6, where our method can precisely predict the missing part of the input while other methods tend to output blurry point cloud in the missing region. Moreover, our method can produce more uniformly-distributed dense point cloud with fewer noises in contrast to other methods, benefited from the IFNet with self-correction procedure.

Results on MVP. Since our method can generate complete point cloud with various resolutions by modifying the upsampling rate r , we compare our method with existing methods that support multi-resolution completion. Except for CD loss, we also use F-Score [14] to evaluate the distance between objects as in [21]. As shown in Tab. 2, our method outperforms all the other methods in terms of both CD and F-Score@1%.

Results on KITTI. Since there are no complete ground truth point clouds for KITTI, we follow the

Tab. 3 Shape completion results on KITTI dataset w.r.t. Fidelity Distance (FD), Minimal Matching Distance (MMD), Consistency, and Uniformity.

Methods	FD ($\times 10^{-3}$)	MMD ($\times 10^{-3}$)	Consistency ($\times 10^{-3}$)	Uniformity		
				0.4%	0.8%	1.2%
PCN [47]	2.235	1.366	1.557	3.662	7.710	10.823
TopNet [29]	5.354	0.636	0.568	1.353	1.219	0.950
MSN [18]	0.434	2.259	1.951	0.822	0.523	0.383
NSFA [49]	1.281	0.891	0.491	0.992	0.767	0.552
PF-Net [11]	1.137	0.792	0.436	0.881	0.682	0.491
CRN [32]	1.023	0.872	0.431	0.870	0.673	0.485
GRNet [42]	0.816	0.568	0.313	0.632	0.489	0.352
VRCNet [21]	2.586	0.378	0.259	0.751	0.582	0.416
SnowflakeNet [40]	0.220	0.664	0.557	0.979	0.730	0.499
ASHF-Net [51]	0.773	0.541	0.298	0.602	0.466	0.335
Ours	0.586	0.336	0.314	0.506	0.313	0.148

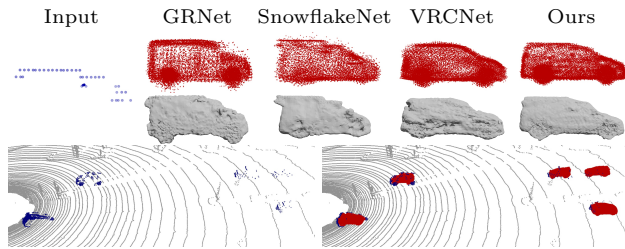


Fig. 7 Qualitative point cloud completion and surface reconstruction results on KITTI dataset.

protocol of ASHF-Net [51] to evaluate the performance, where Fidelity, Minimal Matching Distance (MMD), Consistency and Uniformity are used as evaluation metrics. Tab. 3 shows the advantages of the point clouds generated by our method over the other methods in terms of distribution uniformity, which demonstrates that the proposed IFNet is beneficial to produce uniformly distributed point cloud through the iterative self-correction procedure. Besides, our approach achieves the lowest MMD among all the methods. Other than the quantitative comparison, we also visualize point cloud completion results and surface reconstruction results in Fig. 7, where the mesh is created by Poisson Surface Reconstruction [12]. We can observe that other methods produce more artifacts in the reconstructed surfaces due to the generation of unevenly distributed point set, while our method produce smoother surface and clearer structures in the completion results.

4.4 Ablation Study

We demonstrate the effectiveness of the proposed networks through an ablation study. We conduct all the experiments on ShapeNet dataset and all the experimental settings including the network

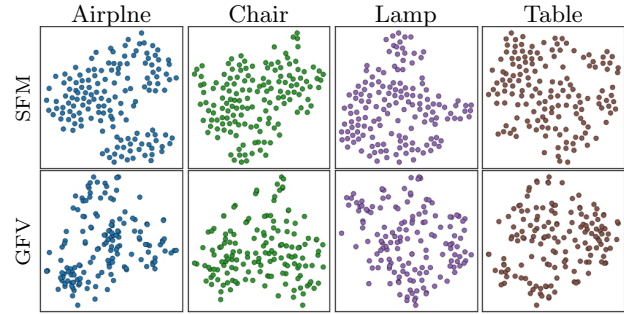


Fig. 8 Compared to GFV used in [40], the feature embedding of the learned *SFM* is more uniformly distributed.

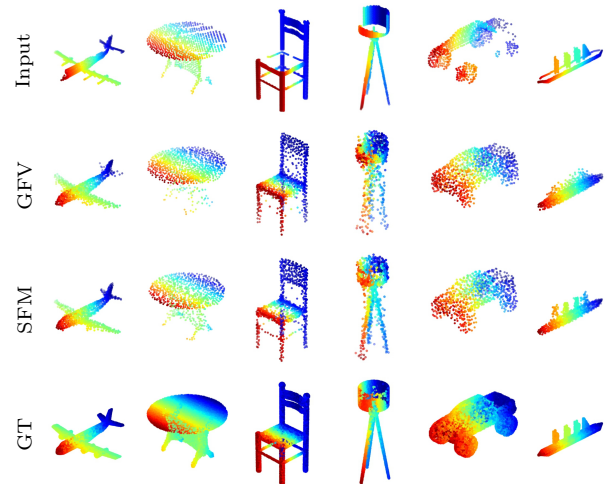


Fig. 9 Visual comparison of coarse point clouds generated from SFM and GFV.

architectures are the same as described in Sec. 4.2, except for the analysis part.

Feature structuring network. We compare the performance of point cloud completion to quantitatively validate the effect of the FSNet, where the structured feature map SFM is generated with different numbers of channels h . Additionally, we replace the FSNet with max-pooling operation to produce a global feature vector (GFV) as the global representation instead of SFM, and the coarse point cloud is generated by the module in previous method [40]. As shown in Tab. 4, the completion quality of SFM-based method for both coarse and dense point clouds is better than GFV-based method. Visual comparison between the coarse point clouds generated with different methods is shown in Fig. 9, and we see that our method can provide complete shape with clearer structures. We also note that CD decreases to the lowest value when h increases to 32, which demonstrates the effectiveness of FSNet. However,

Tab. 4 Shape completion (CD loss multiplied by 10^4) on ShapeNet dataset of GFV-based method and SFM-based method with different numbers of channels.

Methods	CD	
	Coarse	Dense
GFV	9.77	2.64
Ours ($h = 8$)	7.68	2.40
Ours ($h = 16$)	7.62	2.35
Ours ($h = 32$)	7.26	2.27
Ours ($h = 64$)	7.64	2.30

CD increases when h rises to 64, which indicates that although SFM with more number of channels can represent richer latent patterns, it may lead to information redundancy.

Furthermore, We also provide a visualization of learned SFM projection of testing samples in ShapeNet dataset in Fig. 8. Compared with recent GFV based method [40], the distribution of SFM projections is more uniform at instance level across different categories, demonstrating that SFM has learned sufficient local information to distinguish different shapes. Note that we use the same encoder as [40] when conducting the comparison.

Iterative feedback network. Feature expansion is an important component in recent point cloud upsampling methods. However, existing feature expansion methods, including multi-branch MLPs (MB) [45], duplicated-based expansion (DP) [17] and NodeShuffle (NS) [24] generally perform expansion in one or two steps, which limits their performance in point cloud completion task with incomplete and non-uniform inputs. To demonstrate the effectiveness of IFNet, we conduct comparison experiments where IFNet in our pipeline is either replaced with other features expansion methods or composed of different number T of feedback blocks. The quantitative results are shown in Tab. 5. It demonstrates the advantage of IFNet against other methods in point cloud completion task, and the completion quality is improved as the number of feedback blocks increases. Qualitative completion results and their close-ups are illustrated in Fig. 10. It shows that the dense point clouds generated by our method are with fewer outliers and noises, which proves that the proposed IFNet facilitates the consolidation and uniformity of point cloud.

For a more comprehensive understanding of the progressive refinement process in IFNet, we visualize the intermediate completion results in Fig. 11, where

Tab. 5 Shape completion results (CD loss multiplied by 10^4) on ShapeNet dataset with different feature expansion networks.

Methods	Plane	Cabinet	Car	Chair	Lamp	Sofa	Table	Vessel	Avg.
MB [45]	0.99	3.80	2.30	3.64	3.12	4.26	2.77	2.61	2.94
DP [17]	1.00	3.88	2.30	3.46	3.07	4.24	2.75	2.60	2.92
NS [24]	0.96	3.79	2.28	3.23	2.95	4.17	2.68	2.51	2.82
Ours ($T = 1$)	0.80	3.64	2.21	3.05	2.23	3.87	2.31	1.88	2.50
Ours ($T = 3$)	0.79	3.45	2.24	2.86	1.99	3.98	2.27	2.03	2.45
Ours ($T = 5$)	0.82	3.52	2.18	2.97	1.85	3.65	2.12	1.92	2.38
Ours ($T = 7$)	0.84	3.47	2.18	2.63	1.84	3.73	2.04	1.90	2.33
Ours ($T = 9$)	0.80	3.53	2.13	2.48	1.79	3.64	1.98	1.81	2.27

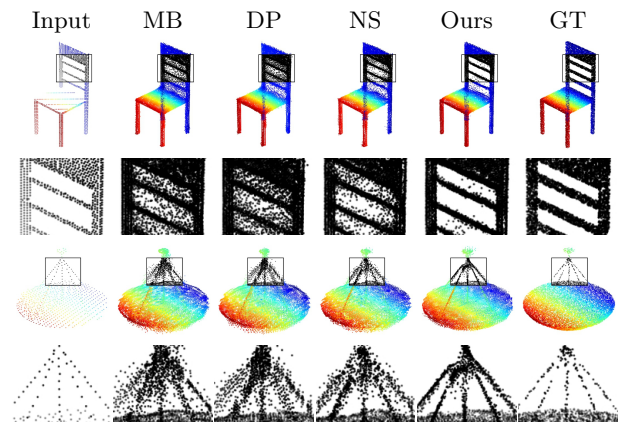


Fig. 10 Visual examples of shape completion results on ShapeNet dataset with different feature expansion networks.

the offsets between the coordinates of points in P^s and the dense point cloud in step t are regressed from the corresponding dense features F_t^d . It shows that as the the dense features are progressively corrected via the feedback mechanism, the local details and surface uniformity of the dense point cloud are gradually improved. Note that only the dense features from the last feedback block are fed to the offset regression module during both the training and test stages, and there is no need to supervise the intermediate results as previous methods do [11, 40].

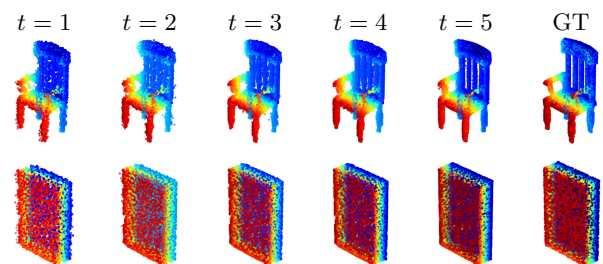


Fig. 11 Visual example of shape completion results on ShapeNet dataset regressed from the intermediate features in IFNet.

5 Conclusion

In this study, we revisit the problem of point cloud completion and propose two novel networks which can be integrated into a coarse-to-fine pipeline. By replacing the max pooling operation with FSNet, we are able to efficiently aggregate both global and local information from the partial observation. Moreover, we introduce IFNet into the upsampling stage, which can work in a self-correction manner and help progressively refine local details of the output shape. Experiments on multiple datasets indicate that our method achieve state-of-the-art performance. However, our method still has certain limitations. FSNet requires extra computation cost compared to the max-pooling operation and it may lead to information redundancy as discussed in the ablation study, while IFNet takes multiple steps to expand the sparse features, which is also relatively time-consuming. It is worth exploring ways to address these limitations and possibility of applying our method to other tasks like point cloud consolidation and upsampling. Moreover, since we use multi-head attention in FSNet and self-attention in IFNet, it is interesting to explore some more sophisticated attention mechanisms [8], e.g., transformer-based modules that have been proven to be helpful in 3D point cloud processing [7, 50], to see if the performance can be further improved.

Acknowledgements

We would like to thank the authors of several important prior methods for making their source code and pre-trained models publicly available.

Open Access This article is distributed under the terms of the Creative Commons Attribution License which permits any use, distribution, and reproduction in any medium, provided the original author(s) and the source are credited.

References

- [1] A. Alliegro, D. Valsesia, G. Fracastoro, E. Magli, and T. Tommasi. Denoise and contrast for category agnostic shape completion. In *Proceedings of the IEEE/CVF Conference on Computer Vision and Pattern Recognition*, pages 4629–4638, 2021.
- [2] I. Armeni, O. Sener, A. R. Zamir, H. Jiang, I. Brilakis, M. Fischer, and S. Savarese. 3d semantic parsing of large-scale indoor spaces. In *Proceedings of the IEEE Conference on Computer Vision and Pattern Recognition*, pages 1534–1543, 2016.
- [3] M. Berger, A. Tagliasacchi, L. Seversky, P. Alliez, J. Levine, A. Sharf, and C. Silva. State of the art in surface reconstruction from point clouds. In *Eurographics 2014-State of the Art Reports*, volume 1(1), pages 161–185, 2014.
- [4] A. Dai, C. R. Qi, and M. Nießner. Shape completion using 3d-encoder-predictor cnns and shape synthesis. In *Proceedings of the IEEE Conference on Computer Vision and Pattern Recognition*, pages 5868–5877, 2017.
- [5] H. Fan, H. Su, and L. J. Guibas. A point set generation network for 3d object reconstruction from a single image. In *Proceedings of the IEEE conference on computer vision and pattern recognition*, pages 605–613, 2017.
- [6] A. Geiger, P. Lenz, C. Stiller, and R. Urtasun. Vision meets robotics: The kitti dataset. *The International Journal of Robotics Research*, 32(11):1231–1237, 2013.
- [7] M.-H. Guo, J.-X. Cai, Z.-N. Liu, T.-J. Mu, R. R. Martin, and S.-M. Hu. Pct: Point cloud transformer. *Computational Visual Media*, 7(2):187–199, 2021.
- [8] M.-H. Guo, T.-X. Xu, J.-J. Liu, Z.-N. Liu, P.-T. Jiang, T.-J. Mu, S.-H. Zhang, R. R. Martin, M.-M. Cheng, and S.-M. Hu. Attention mechanisms in computer vision: A survey. *arXiv preprint arXiv:2111.07624*, 2021.
- [9] M. Haris, G. Shakhnarovich, and N. Ukita. Deep back-projection networks for super-resolution. In *Proceedings of the IEEE conference on computer vision and pattern recognition*, pages 1664–1673, 2018.
- [10] T. Hu, Z. Han, A. Shrivastava, and M. Zwicker. Render4completion: Synthesizing multi-view depth maps for 3d shape completion. In *Proceedings of the IEEE/CVF International Conference on Computer Vision Workshops*, pages 0–0, 2019.
- [11] Z. Huang, Y. Yu, J. Xu, F. Ni, and X. Le. Pf-net: Point fractal network for 3d point cloud completion. In *Proceedings of the IEEE/CVF Conference on Computer Vision and Pattern Recognition*, pages 7662–7670, 2020.
- [12] M. Kazhdan and H. Hoppe. Screened poisson surface reconstruction. *ACM Transactions on Graphics (ToG)*, 32(3):1–13, 2013.
- [13] D. P. Kingma and J. Ba. Adam: A method for stochastic optimization. *arXiv preprint arXiv:1412.6980*, 2014.
- [14] A. Knapitsch, J. Park, Q.-Y. Zhou, and V. Koltun. Tanks and temples: Benchmarking large-scale scene reconstruction. *ACM Transactions on Graphics (ToG)*, 36(4):1–13, 2017.
- [15] T. Kruse, A. K. Pandey, R. Alami, and A. Kirsch. Human-aware robot navigation: A survey. *Robotics and Autonomous Systems*, 61(12):1726–1743, 2013.
- [16] J. Lee, Y. Lee, J. Kim, A. Kosiorok, S. Choi, and Y. W. Teh. Set transformer: A framework for attention-based permutation-invariant neural networks. In *International Conference on Machine Learning*, pages

- 3744–3753. PMLR, 2019.
- [17] R. Li, X. Li, C.-W. Fu, D. Cohen-Or, and P.-A. Heng. Pu-gan: a point cloud upsampling adversarial network. In *Proceedings of the IEEE/CVF International Conference on Computer Vision*, pages 7203–7212, 2019.
- [18] M. Liu, L. Sheng, S. Yang, J. Shao, and S.-M. Hu. Morphing and sampling network for dense point cloud completion. In *Proceedings of the AAAI conference on artificial intelligence*, volume 34(07), pages 11596–11603, 2020.
- [19] N. J. Mitra, M. Pauly, M. Wand, and D. Ceylan. Symmetry in 3d geometry: Extraction and applications. In *Computer Graphics Forum*, volume 32(6), pages 1–23. Wiley Online Library, 2013.
- [20] L. Pan. Ecg: Edge-aware point cloud completion with graph convolution. *IEEE Robotics and Automation Letters*, 5(3):4392–4398, 2020.
- [21] L. Pan, X. Chen, Z. Cai, J. Zhang, H. Zhao, S. Yi, and Z. Liu. Variational relational point completion network. In *Proceedings of the IEEE/CVF Conference on Computer Vision and Pattern Recognition*, pages 8524–8533, 2021.
- [22] C. R. Qi, H. Su, K. Mo, and L. J. Guibas. Pointnet: Deep learning on point sets for 3d classification and segmentation. In *Proceedings of the IEEE conference on computer vision and pattern recognition*, pages 652–660, 2017.
- [23] C. R. Qi, L. Yi, H. Su, and L. J. Guibas. Pointnet++: Deep hierarchical feature learning on point sets in a metric space. *arXiv preprint arXiv:1706.02413*, 2017.
- [24] G. Qian, A. Abualshour, G. Li, A. Thabet, and B. Ghanem. Pu-gcn: Point cloud upsampling using graph convolutional networks. In *Proceedings of the IEEE/CVF Conference on Computer Vision and Pattern Recognition*, pages 11683–11692, 2021.
- [25] Y. Qian, J. Hou, S. Kwong, and Y. He. Pugeonet: A geometry-centric network for 3d point cloud upsampling. In *European Conference on Computer Vision*, pages 752–769. Springer, 2020.
- [26] M. Sarmad, H. J. Lee, and Y. M. Kim. Rl-gan-net: A reinforcement learning agent controlled gan network for real-time point cloud shape completion. In *Proceedings of the IEEE/CVF Conference on Computer Vision and Pattern Recognition*, pages 5898–5907, 2019.
- [27] D. Stutz and A. Geiger. Learning 3d shape completion from laser scan data with weak supervision. In *Proceedings of the IEEE Conference on Computer Vision and Pattern Recognition*, pages 1955–1964, 2018.
- [28] M. Tarini, H. P. Lensch, M. Goesele, and H.-P. Seidel. 3d acquisition of mirroring objects using striped patterns. *Graphical Models*, 67(4):233–259, 2005.
- [29] L. P. Tchapmi, V. Kosaraju, H. Rezatofghi, I. Reid, and S. Savarese. Topnet: Structural point cloud decoder. In *Proceedings of the IEEE/CVF Conference on Computer Vision and Pattern Recognition*, pages 383–392, 2019.
- [30] A. Vaswani, N. Shazeer, N. Parmar, J. Uszkoreit, L. Jones, A. N. Gomez, L. Kaiser, and I. Polosukhin. Attention is all you need. In *Advances in neural information processing systems*, pages 5998–6008, 2017.
- [31] X. Wang, M. H. Ang, and G. H. Lee. Voxel-based network for shape completion by leveraging edge generation. In *Proceedings of the IEEE/CVF International Conference on Computer Vision*, pages 13189–13198, 2021.
- [32] X. Wang, M. H. Ang Jr, and G. H. Lee. Cascaded refinement network for point cloud completion. In *Proceedings of the IEEE/CVF Conference on Computer Vision and Pattern Recognition*, pages 790–799, 2020.
- [33] Y. Wang, Y. Sun, Z. Liu, S. E. Sarma, M. M. Bronstein, and J. M. Solomon. Dynamic graph cnn for learning on point clouds. *Acm Transactions On Graphics (tog)*, 38(5):1–12, 2019.
- [34] Y. Wang, D. J. Tan, N. Navab, and F. Tombari. Softpoolnet: Shape descriptor for point cloud completion and classification. In *Computer Vision—ECCV 2020: 16th European Conference, Glasgow, UK, August 23–28, 2020, Proceedings, Part III 16*, pages 70–85. Springer, 2020.
- [35] X. Wen, Z. Han, Y.-P. Cao, P. Wan, W. Zheng, and Y.-S. Liu. Cycle4completion: Unpaired point cloud completion using cycle transformation with missing region coding. In *Proceedings of the IEEE/CVF Conference on Computer Vision and Pattern Recognition*, pages 13080–13089, 2021.
- [36] X. Wen, T. Li, Z. Han, and Y.-S. Liu. Point cloud completion by skip-attention network with hierarchical folding. In *Proceedings of the IEEE/CVF Conference on Computer Vision and Pattern Recognition*, pages 1939–1948, 2020.
- [37] X. Wen, P. Xiang, Z. Han, Y.-P. Cao, P. Wan, W. Zheng, and Y.-S. Liu. Pmp-net: Point cloud completion by learning multi-step point moving paths. In *Proceedings of the IEEE/CVF Conference on Computer Vision and Pattern Recognition*, pages 7443–7452, 2021.
- [38] Z. Wu, S. Song, A. Khosla, F. Yu, L. Zhang, X. Tang, and J. Xiao. 3d shapenets: A deep representation for volumetric shapes. In *Proceedings of the IEEE conference on computer vision and pattern recognition*, pages 1912–1920, 2015.
- [39] Y. Xia, Y. Xia, W. Li, R. Song, K. Cao, and U. Stilla. Asfm-net: Asymmetrical siamese feature matching network for point completion. *arXiv preprint arXiv:2104.09587*, 2021.
- [40] P. Xiang, X. Wen, Y.-S. Liu, Y.-P. Cao, P. Wan, W. Zheng, and Z. Han. Snowflakenet: Point cloud completion by snowflake point deconvolution with skip-transformer. In *Proceedings of the IEEE/CVF International Conference on Computer Vision*, pages

- 5499–5509, 2021.
- [41] C. Xie, C. Wang, B. Zhang, H. Yang, D. Chen, and F. Wen. Style-based point generator with adversarial rendering for point cloud completion. In *Proceedings of the IEEE/CVF Conference on Computer Vision and Pattern Recognition*, pages 4619–4628, 2021.
- [42] H. Xie, H. Yao, S. Zhou, J. Mao, S. Zhang, and W. Sun. Grnet: Gridding residual network for dense point cloud completion. In *European Conference on Computer Vision*, pages 365–381. Springer, 2020.
- [43] W. Yifan, S. Wu, H. Huang, D. Cohen-Or, and O. Sorkine-Hornung. Patch-based progressive 3d point set upsampling. In *Proceedings of the IEEE/CVF Conference on Computer Vision and Pattern Recognition*, pages 5958–5967, 2019.
- [44] L. Yu, X. Li, C.-W. Fu, D. Cohen-Or, and P.-A. Heng. Ec-net: an edge-aware point set consolidation network. In *Proceedings of the European Conference on Computer Vision (ECCV)*, pages 386–402, 2018.
- [45] L. Yu, X. Li, C.-W. Fu, D. Cohen-Or, and P.-A. Heng. Pu-net: Point cloud upsampling network. In *Proceedings of the IEEE Conference on Computer Vision and Pattern Recognition*, pages 2790–2799, 2018.
- [46] X. Yu, Y. Rao, Z. Wang, Z. Liu, J. Lu, and J. Zhou. Pointr: Diverse point cloud completion with geometry-aware transformers. In *Proceedings of the IEEE/CVF International Conference on Computer Vision*, pages 12498–12507, 2021.
- [47] W. Yuan, T. Khot, D. Held, C. Mertz, and M. Hebert. Pcn: Point completion network. In *2018 International Conference on 3D Vision (3DV)*, pages 728–737. IEEE, 2018.
- [48] H. Zhang, I. Goodfellow, D. Metaxas, and A. Odena. Self-attention generative adversarial networks. In *International conference on machine learning*, pages 7354–7363. PMLR, 2019.
- [49] W. Zhang, Q. Yan, and C. Xiao. Detail preserved point cloud completion via separated feature aggregation. In *Computer Vision—ECCV 2020: 16th European Conference, Glasgow, UK, August 23–28, 2020, Proceedings, Part XXV 16*, pages 512–528. Springer, 2020.
- [50] H. Zhao, L. Jiang, J. Jia, P. H. Torr, and V. Koltun. Point transformer. In *Proceedings of the IEEE/CVF International Conference on Computer Vision*, pages 16259–16268, 2021.
- [51] D. Zong, S. Sun, and J. Zhao. Ashf-net: Adaptive sampling and hierarchical folding network for robust point cloud completion. In *Proceedings of the AAAI Conference on Artificial Intelligence*, volume 35(4), pages 3625–3632, 2021.